Markov-based Channel Characterization for Tractable Performance Analysis in Wireless Packet Networks*

Mohamed Hassan[§], Marwan Krunz[§], and Ibrahim Matta[§§]

[§]Department of Electrical & Computer Engineering

University of Arizona, Tucson, AZ 85721

{mhassan, krunz}@ece.arizona.edu

[§§]Department of Computer Science

Boston University, Boston, MA 02215

matta@cs.bu.edu

Last updated: December 20, 2002

Abstract

Finite-state Markov chain (FSMC) models have often been used to characterize the wireless channel. The fitting is typically performed by partitioning the range of the received signal-to-noise ratio (SNR) into a set of intervals (states). Different partitioning criteria have been proposed in the literature, but none of them was targeted to facilitating the analysis of the packet delay and loss performance over the wireless link. In this paper, we propose a new partitioning approach that results in a FSMC model with tractable queueing performance. Our approach utilizes Jake's level-crossing analysis, the distribution of the received SNR, and the elegant analytical structure of Mitra's producer-consumer fluid queueing model [16]. An algorithm is provided for computing the various parameters of the model, which are then used in deriving closed-form expressions for the *effective bandwidth* (EB) subject to packet loss and delay constraints. Resource allocation based on the EB is key to improving the *perceived* capacity of the wireless medium. Numerical investigations are carried out to study the interactions among various key parameters, verify the adequacy of the analysis, and study the impact of error control parameters on the allocated bandwidth for guaranteed packet loss and delay performance.

keywords — Markov modeling, wireless channels, Rayleigh fading, performance analysis.

*This work was supported in part by the National Science Foundation under grants ANI-9733143, CCR-9979310, and ANI-0095626, and by the Center for Low Power Electronics (CLPE) at the University of Arizona. An abridged version of this paper was presented at the *MMT '02 Workshop*, Rennes, France, June 2002. M. Krunz is the correspondence author.

1 Introduction

Wireless networks are characterized by time-varying channels whose bit error rates (BERs) vary dramatically according to the received SNR. Due to their mathematical tractability, finite-state Markov chain (FSMC) models have often been used to characterize the BER behavior [1, 2, 3]. Typically, an FSMC model is constructed by partitioning the range of the received SNR into a set of non-overlapping intervals $[0, r_1), [r_1, r_2), \ldots [r_i, r_{i+1}), \ldots [r_N, \infty)$. Each interval is represented by a nominal BER, which in turn represents a certain channel quality. In our study, the selection of the thresholds $r_i,\ i = 1, \ldots, N$, and their corresponding nominal BERs is done in a manner that leads to tractable analysis of the packet loss and delay performance over the wireless link.

Several studies have addressed the modeling of the wireless channel through appropriate partitioning of the received SNR [6, 7, 8, 9, 10]. In [6] a Markov model was presented based on experimental measurements of real channels. To maximize the throughput while minimizing the probability of packet error, Rice and Wicker [7] represented the time-varying channel by a FSMC model in which the thresholds $r_i, i = 0, 1, \ldots N$, were obtained by counting the number of retransmission requests during the so-called *observation* or *frame intervals*. In [8] a FSMC model was constructed by optimizing the system performance in the sense of maximizing the channel capacity. By requiring all states to have the same mean durations, Zhang and Kassam [9] employed a FSMC model for the Rayleigh fading channel. Using the Nakagami-m distributions as the basis for partitioning, the authors in [10] characterized the dynamics of amplitude variations of time-varying multi-path fading. They also built a FSMC model whose states represent the different intervals of fading amplitude. None of the above models was designed to enable tractable analysis of *packet-level* performance degradations. More specifically, the use of packet buffering at the transmitter side of a wireless link introduces variable queueing delays and occasional packet loss (due to buffer overflow). Prior assessment of such degradations is a key to providing QoS guarantees and to the design of online admission control policies. Hence, a *good* model should not only reflect the physical characteristics of the channel, but it should also facilitate analytical investigation of its performance.

A key problem in the design of wireless networks is how to efficiently allocate their scarce resources to meet applications' packet loss and delay requirements. Such efficient allocation can be achieved using the concept of *effective bandwidth* (EB). In general, the EB refers to the minimum amount of network resources (in bits per second) that if allocated to a given traffic flow would guarantee a certain level of

QoS (typically, in terms of the packet loss rate). The EB has been extensively studied for wireline packet networks and has been widely accepted as a basis for connection admission control (CAC) and resource allocation (e.g., [14, 18, 22, 26, 23, 25]). In [11, 15] the authors presented an analytical framework for studying the packet loss and delay performance over a wireless link. Based on this framework, they derived closed-form expressions for the EB subject to packet loss and delay constraints. The analysis, however, was conducted under the assumption of a two-state FSMC channel model (a slightly more general version of the Gilbert-Elliot model). Arguably, a two-state model provides a coarse approximation of the channel behavior, and may not always be acceptable. In fact, as shown in this paper, a two-state model leads to a highly conservative (and unnecessary) estimate of the EB. Therefore, the motivation behind our study is to construct a multi-state FSMC model that lends itself to analytical investigation of the EB in the wireless environment.

The main contributions of this paper are twofold. First, we devise a new partitioning approach of the received SNR range that leads to an analytically tractable, multi-state Markov channel model. Second, we use this model to derive closed-form expressions for the EB subject to either packet loss or packet delay constraints. Such expressions can be instrumented in the CAC module at a base station of a cellular network to determine *online* the admissibility of an incoming call request. Our numerical results indicate that such use of the EB results in a significant bandwidth gain.

The rest of the paper is organized as follows. Section 2 presents our analytical framework. In Section 3 we present the adopted SNR partitioning approach. Section 4 provides the queueing model and the corresponding wireless effective bandwidth analysis. Section 5 reports the numerical results. Finally, Section 6 summarizes the results of this study and outlines our future work.

2 Wireless-Link Model

2.1 Preliminaries

Consider Figure 1, which represents a simplified representation of a wireless link. Arriving packets at the transmitter are stored temporarily in a FIFO buffer, which is drained at a rate that depends on the state of the channel at the receiver. Throughout this work, we refer to the draining (or service) rate when the received SNR is r by $c(r)$. After departing the buffer, a packet undergoes a strong CRC encoding followed by partial FEC that allows for correcting only a fraction of packet errors. This hybrid ARQ approach

is often used to enhance the efficiency of the wireless link by minimizing the number of retransmissions. In practice, the transmission path also includes packet and bit interleavers, possibly in conjunction with multiple FEC encoders (e.g., outer and inner encoders). For simplicity, we do not directly account for the impact of interleaving, but assume that such impact has already been incorporated in the FEC "box" in Figure 1. In other words, this box could consist of multiple stages of encoding and interleaving.

In packet networks, a traffic source is often viewed as an alternating sequence of active and idle periods. During an active period, one or more network-layer packets (e.g., IP datagrams) arrive back-to-back, forming a burst (an active period). This so-called on/off model has the advantage of being able to capture the bursty nature of various types of network traffic, including computer data, voice, and VBR video [12]. Its appropriateness in analyzing the performance over wireless links was demonstrated in several previous studies (e.g., [11, 13]). When a network-layer packet arrives at a transmitting node, it is typically fragmented into fixed-size *link-layer* (LL) packets that are then transmitted over the wireless interface. The sheer difference between the burst and LL-packet time scales makes it reasonable to separate the two by adopting a *fluid* approximation of the arrival traffic. Such a decomposition approach, which has been successfully applied in wireline networks [16, 18, 20, 14], allows us to emphasize the time scale of most relevance to network-layer performance (e.g., packet loss rate and queueing delay).

Accordingly, we consider M incoming traffic sources, each of which is modeled as a fluid source with exponentially distributed on and off periods. The means of the on and off periods are $1/\alpha$ and $1/\beta$, respectively. When the source is active, it transmits at a peak rate σ. The channel is modeled by the $(N+1)$-state FSMC model shown in Figure 2. This particular structure of the Markov chain is chosen because it lends itself to the queueing analysis of Mitra's producer-consumer model [16] (to be described later), which allows us to evaluate the packet loss and delay performance over the wireless channel and compute closed-form expressions for the EB.

Let π_i be the steady-state probability that the channel is in state i, $i = 0, \ldots, N$. The FSMC stays in state i for an exponentially distributed time with mean T_i. It is assumed that bit errors within any given state are mutually independent. For an FEC code with a correction capability of τ bits per code block (packet), the probability of an uncorrectable error in a received packet when the channel is in state i is given by:

$$P_{c_i} = \sum_{j=\tau+1}^{n} \binom{n}{j} (P_e(\hat{r}_i))^j \, (1 - P_e(\hat{r}_i))^{n-j} \tag{1}$$

where n is the number of bits in a code block, including the FEC bits, $P_e(r)$ is the BER when the instantaneous SNR is r (the form of $P_e(r)$ depends on the underlying modulation scheme), and $\hat{r}_i$ is the "nominal" SNR value in state i (its calculation will be discussed later). The packet transmission/retransmission process can be approximated by a Bernoulli process [1]. We assume that the transmitter always gets the feedback message from the receiver before the next transmission slot, and a packet is retransmitted persistently until it is successfully received. The *nominal* service rate in state i, denoted by c_i, can be approximated by the inverse of the mean of the geometrically distributed retransmission process:

$$c_i = c.e.(1 - P_{c_i}), \qquad i = 0, 1, 2, \ldots, N \tag{2}$$

where c is the error-free service rate, $e = k/n$ is the FEC overhead, and k is the number of information bits in a code block. We take $c_0 = 0$ (the nominal service rate during the worst state).

Wireless transmission of continuous waveforms in obstacle environments is prone to multi-path fading, which results in randomly varying envelope for the received signal. This randomness has been shown to follow a Rayleigh distribution. In the presence of additive Gaussian noise, the instantaneous received SNR r is proportional to the square of the signal envelope [5]. Accordingly, the SNR is exponentially distributed with pdf:

$$p_R(r) = \frac{1}{\rho} e^{\frac{-r}{\rho}}, \quad r > 0 \tag{3}$$

where $\rho \stackrel{\text{def}}{=} E[r]$. An important parameter that reflects the behavior of the SNR process at the receiver is the level-crossing rate (LCR), defined as the average rate at which the signal envelope crosses a given SNR level r. For the Rayleigh fading channel, the LCR at an instantaneous SNR r is given by [5]:

$$L(r) = \sqrt{\frac{2\pi r}{\rho}} f_m e^{\frac{-r}{\rho}} \tag{4}$$

where $f_m = \frac{f_o v}{w}$ is the Doppler frequency, w is the speed of the electromagnetic wave, v is the speed of the mobile user, and f_o is the carrier frequency. We assume slow fading with respect to symbol transmission time. Furthermore, we assume that transitions between channel states take place only at the end of a packet transmission. As mentioned before, the FSMC model that represents the time-varying behavior of

the Rayleigh fading channel will be obtained by partitioning the received SNR into $N+1$ intervals (states). Let $r_0 = 0 < r_1 < r_2 < \ldots < r_{N-1} < r_N < r_{N+1} = \infty$ be the $N+2$ thresholds that define the partitioning. The steady-state probability that the FSMC is in state i is given by:

$$\pi_i = \int_{r_i}^{r_{i+1}} \frac{1}{\rho} e^{\frac{-r}{\rho}} dr = e^{\frac{-r_i}{\rho}} - e^{\frac{-r_{i+1}}{\rho}} \tag{5}$$

2.2 Mitra's Producers-Consumers Fluid Model

In this section, we briefly describe Mitra's producers-consumers fluid queueing model [16]. This model facilitates the analytical investigation of communication systems possessing randomly varying statistical properties. According to this model, the fluid produced by M producers is supplied to a FIFO buffer that is drained by N consumers. Each producer and consumer alternates between independent and exponentially distributed active and idle periods. Let λ^{-1} and μ^{-1} denote the mean of the idle and active periods of a consumer, respectively. When active, a consumer drains fluid from the buffer at a constant rate, which is the same for all consumers. It is easy to see that the number of active consumers fluctuates in time according to the Markov chain in Figure 2. In [16] Mitra analyzed the steady-state behavior of this queueing system. We use his analysis as the basis to derive the wireless EB. In our wireless model, M corresponds to the number of incoming ON/OFF sources at the transmitting node, while N corresponds to the ratio between the *nominal* service rate when the channel is in the best state (state N) and the corresponding service rate when the channel is in the second worst state (state 1). (recall that the nominal service rate in state 0 is zero). In other words, one can think of the nominal service rate in state 1 as the unit of bandwidth, and of N as the number of units of bandwidth that can be offered when the channel is in the best state.

To analyze the packet loss and delay performance, we must first partition the wireless channel in a manner that produces the same Markovian structure of Figure 2. In other words, we match the service rate at the transmitter buffer to the *total* instantaneous consumption rate in Mitra's model. This requires that we choose the partitioning thresholds such that each state corresponds to a given number of active consumers. Let $\theta(r) \stackrel{\text{def}}{=} \frac{c(r)}{c(\infty)}$ be the ratio between the service rate at a received SNR r and its value when the channel is error-free (note that $c(\infty) < c$ due to the FEC overhead). We form a FSMC model based on the requirement that in each SNR interval $[r_i, r_{i+1})$, there exists a point $\hat{r_i}$, $r_i \leq \hat{r_i} < r_{i+1}$, that satisfies

the following relationship:

$$\theta(\hat{r}_i) \stackrel{\text{def}}{=} \frac{c(\hat{r}_i)}{c(\infty)} = \frac{i}{N}, \qquad i = 0, 1, \ldots, N-1 \tag{6}$$

Note that in the producer-consumer model, the consumption rate in state i, $i = 0, 1, \ldots, N$, is i times the consumption rate in state 1. The BER that corresponds to $\hat{r}_i$ is called the *nominal* BER associated with state i. We set $\theta(\hat{r}_0) = \theta(r_0) = 0$ and $\theta(\hat{r}_N) = \theta(\infty) = 1$ (i.e., $\hat{r}_N = r_{N+1} = \infty$).

When $N = 1$, the model defaults to the standard 2-state Gilbert-Elliot model with $\theta(\hat{r}_0) = 0$ and $\theta(\hat{r}_1) = 1$, and no partitioning is needed. Hereafter, we concentrate on the case $N \geq 2$.

3 SNR Partitioning

It is easy to see that in the producer-consumer model, the steady-state probability distribution is binomial, i.e.,

$$\pi_i = \left(\begin{array}{c} N \\ i \end{array} \right) \left(\frac{\lambda}{\mu}\right)^i \frac{1}{\left(1 + \frac{\lambda}{\mu}\right)^N}, \quad i = 0, \ldots, N \tag{7}$$

For our wireless channel to fit the Markov chain in [16], the partitioning must be done so that no more than one state falls in the "good" (BER close to zero) and "bad" (BER close to one) regions of the SNR space, since either scenario will lead to an unrealistic number of states. This can be justified as follows. For $i = 1, \ldots, N$, $\hat{r}_i$ must satisfy (6). Selecting two states in the "bad" region implies that

$$\frac{1}{N} = \theta(\hat{r}_1) < \theta(r_2) \ll 1$$

which results in a very large N. Likewise, selecting two states in the "good" region will lead to:

$$\theta(\hat{r}_{N-1}) \geq \theta(r_{N-1}) = 1 - \epsilon$$

where $0 < \epsilon \ll 1$. Hence,

$$\frac{N-1}{N} \geq 1 - \epsilon$$

which also leads to a large N.

To completely specify the underlying Markov chain, we need to determine N, $\frac{\lambda}{\mu}$, and the thresholds $r_1, r_2, \ldots, r_N$. Our procedure for computing these quantities is outlined as follows. First, by equating (5)

and (7), we get an expression for N in terms of r_1 and $\frac{\lambda}{\mu}$. Using the level-crossing analysis and the structure of the embedded Markov chain, we then obtain an expression for $\frac{\lambda}{\mu}$ in terms of r_1 and r_N. Combining the obtained expressions, we can express N in terms of r_1 and r_N only. Then, by selecting an appropriate value for r_N, the value of the threshold r_1 can be obtained. After obtaining r_1, the other thresholds can be obtained recursively, as follows: The steady-state probability that the channel is in state i is given by (5), from which and after obtaining the ith threshold r_i, the $(i+1)$th threshold can be obtained using the following expression:

$$r_{i+1} = -\rho \ln(e^{\frac{-r_i}{\rho}} - \pi_i), \quad i = 1, 2, \ldots, N-2 \tag{8}$$

The details of the above procedure are now presented. Let $\{X(t) : t \geq 0\}$ be the (irreducible) Markov process that represents the state of the channel. The time spent in any state s_i is exponentially distributed with mean $T_i = \frac{1}{q_i}$. The parameter q_i represents the total rate out of state s_i. Consider states 0 and N in Figure 2. The total rate out of state 0 can be approximated by the level-crossing rate (LCR) at r_1, i.e.,

$$N\lambda = L(r_1) = \sqrt{\frac{2\pi r_1}{\rho}} f_m e^{\frac{-r_1}{\rho}} \tag{9}$$

Similarly, the total rate out of state N can be approximated by the LCR at r_N:

$$N\mu = L(r_N) = \sqrt{\frac{2\pi r_N}{\rho}} f_m e^{\frac{-r_N}{\rho}} \tag{10}$$

Dividing (9) by (10), we get the following expression for $\frac{\lambda}{\mu}$:

$$\frac{\lambda}{\mu} = \sqrt{\frac{r_1}{r_N}} \frac{e^{\frac{-r_1}{\rho}}}{e^{\frac{-r_N}{\rho}}} \tag{11}$$

The above equation relates $\frac{\lambda}{\mu}$, r_1, and r_N. We still need to relate N to these parameters. This can be done as follows. From (7), the steady-state probability that the channel is in state 0 is given by:

$$\pi_0 = \frac{1}{\left(1 + \frac{\lambda}{\mu}\right)^N} \tag{12}$$

From (5) π_0 is also given by:

$$\pi_0 = 1 - e^{\frac{-r_1}{\rho}} \tag{13}$$

(recall that $r_0 \stackrel{\text{def}}{=} 0$). From (12) and (13), we have

$$N = -\frac{\ln\left(1 - e^{\frac{-r_1}{\rho}}\right)}{\ln\left(1 + \frac{\lambda}{\mu}\right)} \tag{14}$$

Similarly, the steady-state probability that the channel is in state N is given by:

$$\pi_N = \left(\frac{\lambda}{\mu}\right)^N \left(1 - e^{\frac{-r_1}{\rho}}\right) \tag{15}$$

From (5), and noting that $r_{N+1} \stackrel{\text{def}}{=} \infty$, π_N can also be written as

$$\pi_N = e^{\frac{-r_N}{\rho}} \tag{16}$$

From (15) and (16), an expression for the ratio $\frac{\lambda}{\mu}$ in terms of r_1, r_N, and N can be obtained:

$$\frac{\lambda}{\mu} = \left(\frac{e^{\frac{-r_N}{\rho}}}{1 - e^{\frac{-r_1}{\rho}}}\right)^{\frac{1}{N}} \tag{17}$$

From (15), (16), and (11), we can write the following equation for π_N:

$$\pi_N = e^{\frac{-r_N}{\rho}} = \left(\sqrt{\frac{r_1}{r_N}} \frac{e^{\frac{-r_1}{\rho}}}{e^{\frac{-r_N}{\rho}}}\right)^N \left(1 - e^{\frac{-r_1}{\rho}}\right)$$

Taking the logarithm of both sides, we end up with:

$$\frac{-r_N}{\rho} = N \ln\left(\sqrt{\frac{r_1}{r_N}} \frac{e^{\frac{-r_1}{\rho}}}{e^{\frac{-r_N}{\rho}}}\right) + \ln\left(1 - e^{\frac{-r_1}{\rho}}\right) \tag{18}$$

To explicitly express N in terms of r_1 and r_N, we replace $\frac{\lambda}{\mu}$ in (14) by its expression in (11). Equation (18) can now be solved to obtain r_1 provided that a suitable r_N is chosen. Recall that by a suitable r_N, we mean a value that will not lead to the situation of two states both being in the good or in the bad regions. By arranging the terms in (18), we arrive at the following nonlinear equations that can be solved

numerically for r_1 and N (assuming that ρ and r_N are already known):

$$f(r_1, r_N, N) \stackrel{\text{def}}{=} \frac{r_N}{\rho} + N \ln\left(\sqrt{\frac{r_1}{r_N}} \frac{e^{\frac{-r_1}{\rho}}}{e^{\frac{-r_N}{\rho}}}\right) + \ln\left(1 - e^{\frac{-r_1}{\rho}}\right) = 0 \tag{19}$$

$$N = \frac{-\ln\left(1 - e^{\frac{-r_1}{\rho}}\right)}{\ln\left(1 + \sqrt{\frac{r_1}{r_N}} \frac{e^{\frac{-r_1}{\rho}}}{e^{\frac{-r_N}{\rho}}}\right)}, \quad N \geq 2 \tag{20}$$

In our analysis, we choose r_N such that the service rate at state N is almost equal to the error-free service rate (this depends on the relationship between the SNR and the BER, which in turn is dependent on the modulation scheme). This is done by solving for r_N in

$$\theta(r_N) = \sum_{j=0}^{\tau} \binom{n}{j} P_e^j(r_N)(1 - P_e(r_N))^{n-j} = 1 - \epsilon^* \tag{21}$$

where $0 < \epsilon^* \ll 1$ is a predefined control parameter. In (21) the expression for $P_e(r)$ depends on the deployed modulation scheme. Using the obtained r_N, we numerically solve (19) for r_1. Then from r_1 and r_N we get N using (20). Figure 3-a depicts $f(r_1, r_N, N)$ as a function of r_1 for different values of r_N (with $\rho = 4$). It is easy to show that as $r_1 \to 0$, f approaches $-\infty$. Since f is continuous in r_1, a sufficient condition for the existence of a solution for (19) in the range $(0, r_N]$ is that $\lim_{r_1 \to r_N} f(r_1, r_N, N) \geq 0$. This limit is given by

$$\lim_{r_1 \to r_N} f(r_1, r_N, N) = \frac{r_N}{\rho} + \ln\left(1 - e^{-r_N/\rho}\right) \tag{22}$$

Accordingly, a solution for (19) is guaranteed to exist if $r_N \geq \rho \ln 2$. This gives a lower bound on the value of r_N that is needed to ensure the existence of a solution. Part-b of Figure 3 depicts r_1 resulting from the partitioning versus ρ for various values of r_N. For a given r_N, increasing ρ results in a larger r_1, and subsequently smaller N (the function $\theta(r)$ saturates faster). As shown in part-c of the figure, for a fixed ρ, an increase in r_N results in a decrease in r_1. This, in effect, leads to a larger separation between r_1 and r_N on the SNR axis, and consequently to a higher N value.

The algorithm in Figure 4 summarizes the steps that are needed to obtain the parameters of the FSMC model. Note that the procedure **Parameterize-FSMC** takes as inputs the parameters of the coding scheme (n, k, τ), the modulation-dependent BER function $P_e(.)$, ρ, and ϵ^*. It returns the number of states N, the partitioning thresholds $r_1, \ldots, r_N$, and the nominal SNR values $\hat{r}_1, \ldots, \hat{r}_{N-1}$ (recall that $r_0 = \hat{r}_0 = 0$

and $r_{N+1} = \hat{r}_N = \infty$).

Note that in step 9 of the algorithm if $\theta(r_i) > i/N$ for some state $i \in \{1, 2, \ldots, N-1\}$, then there is no $\hat{r}_i \in [r_i, r_{i+1})$ for which $\theta(\hat{r}_i) = i/N$, and the partitioning does not fulfill the requirements of the producer-consumer model. If that happens, we decrement the value of N and repeat the computations (intuitively, decrementing N increases the ranges of the various states, which improves the likelihood of finding appropriate nominal SNR values). The recursion in step 8 is obtained from $\pi_i = e^{\frac{-r_i}{\rho}} - e^{\frac{-r_{i+1}}{\rho}}$. Note that the algorithm is guaranteed to return a solution, since for $N = 1$ the two nominal SNR values, $\hat{r}_0$ and $\hat{r}_1$, are given (the partitioning reduces to the two-state Gilbert-Elliot model).

4 Performance Analysis

4.1 Queueing Model

Once the parameters of the FSMC are obtained, we proceed to compute the queueing performance. The underlying queueing model can be described by a $(M+1)(N+1)$-state Markov chain. The state space of this chain is given by $S = \{(i, j) : i = 0, \ldots, M \text{ and } j = 0, 1, 2, \ldots, N\}$, where a state (i, j) indicates that there are i active sources and the channel is in state j. Recall that the transition rates for the FSMC are chosen such that the analysis in [17, 16] stays applicable.

The evolution of the buffer content follows the following first-order differential equation [17]:

$$\frac{d\mathbf{\Pi}(\mathbf{x})}{dx}\mathbf{D} = \mathbf{\Pi}(\mathbf{x})\mathbf{M} \tag{23}$$

where $\mathbf{M}$ is the generator matrix of the underlying Markov chain, $\mathbf{D}$ is the diagonal drift matrix, and $\mathbf{\Pi}$ is the probability distribution vector for the buffer content, defined as:

$$\mathbf{\Pi}(x) = [\ \pi_{0,0} \quad \ldots \quad \pi_{0,N} \quad \pi_{1,0} \quad \ldots \quad \pi_{1,N}\ ] \tag{24}$$

$$\pi_{s,i}(x) = \Pr\{Q \leq x, \text{ system is in state } (s, i)\}$$

where Q is the queue length at steady state.

Throughout the paper, boldfaced notation is used to indicate matrices and vectors. The solution of (23) is generally given by the following spectral decomposition:

$$\mathbf{\Pi}(x) = \sum_{z_i \geq 0} a_i e^{-z_i x} \boldsymbol{\phi}_i \tag{25}$$

where a_i's are constant coefficients, and the pairs (z_i, ϕ_i), $i = 1, 2, 3, \ldots$, are the eigenvalues and left eigenvectors of the matrix $\mathbf{MD^{-1}}$ (see [17, 16] for details).

4.2 Wireless Effective Bandwidth

Determining the effective bandwidth amounts to determining the minimum value of c (the error-free service rate before accounting for the FEC overhead) that guarantees a desired QoS requirement. In this section, we determine the wireless EB subject to packet loss and delay constraints. The computation of this EB has been performed in [11, 15] *for the case of a two-state* channel model. As we show later on, this results in an unnecessarily conservative allocation of network bandwidth.

For the packet loss case, the QoS requirement is given by the (x, p) where $\Pr[Q > x] = p$. The corresponding EB is defined by:

$$c^*_{loss} \stackrel{\text{def}}{=} \min\{c \text{ that results in } \Pr[Q > x] = p\} \tag{26}$$

Similarly, in the case of the delay requirement, the EB is defined as:

$$c^*_{delay} \stackrel{\text{def}}{=} \min\{c : \text{ that results in } \Pr[delay > t] = \epsilon_d\} \tag{27}$$

where the pair (t, ϵ_d) represents the delay constraint. Henceforth, we use c^* to indicate either c^*_{loss} or c^*_{delay}, depending on the context. We obtain both quantities in terms of the source, the channel, and the error control parameters.

A common approximation for the EB, which becomes exact as the buffer size goes to infinity, is based on the dominant eigenvalue, z^*, in (25). Essentially, z^* is the eigenvalue with the smallest positive real part. In [14] it is shown that z^* is the unique positive solution for the following equation:

$$\Lambda_A(z) + \Lambda_C(-z) = 0 \tag{28}$$

where $\Lambda_A(z)$ and $\Lambda_c(z)$ are the Gärtner-Ellis limits for the accumulative arrival process $\{A(t) : t \geq 0\}$ and

the accumulative service process $\{C(t) : t \geq 0\}$, respectively, defined as

$$\Lambda_A(z) \stackrel{\text{def}}{=} \limsup_{t\to\infty} t^{-1} \log E[\exp(zA(t))]$$

and similarly for Λ_C. Given z^*, as the buffer size goes to infinity the probability distribution functions for buffer overflow and packet delay are approximately given by [18, 14, 15]:

$$G(x) \stackrel{\text{def}}{=} \Pr[Q > x] \quad = \quad e^{-z^* x} \tag{29}$$

$$\Pr[delay > t] = \epsilon_d \quad = \quad e^{\Lambda_C(-z^*)t} \tag{30}$$

For an aggregate of M two-state sources, $\Lambda_A(z)$ is given by [14]:

$$\Lambda_A(z) \stackrel{\text{def}}{=} \frac{M}{2}\left(-\alpha - \beta + \sigma z + \sqrt{(\alpha + \beta - \sigma z)^2 + 4\beta\sigma z}\right) \tag{31}$$

Recall that $1/\alpha$ and $1/\beta$ are the means of the on and off periods of the incoming traffic flow, respectively, and σ is the peak source rate.

As for the multi-state service process, it can be viewed as a "negative-flow" arrival process, where each consumer represents a fictitious flow with arrival rate that alternates between zero and $-c_1$. Since the N negative-flow sources are independent, $\Lambda_C(z)$ for the total consumption process is given by (Lemma 9.2.1 [14]):

$$\Lambda_C(-z) \stackrel{\text{def}}{=} \sum_{i=1}^{N} \Lambda_{C_i}(-z) = N\Lambda_{C_i}(-z) \tag{32}$$

where $\Lambda_{C_i}(-z)$ is the Gärtner-Ellis limit for one consumer, and is given by:

$$\Lambda_{C_i}(-z) \stackrel{\text{def}}{=} \frac{1}{2}\left(-\lambda - \mu - c_1 z + \sqrt{(\lambda + \mu + c_1 z)^2 - 4\lambda c_1 z}\right) \tag{33}$$

Using (28), (31), and (33), one can solve for z^*. As shown in Appendix I, z^* is found to be one of the roots of a quadratic polynomial in z (hence, it is given in closed form).

Next, we compute c^*_{loss}. Let $\eta \stackrel{\text{def}}{=} c_1/c = e/N = k/(nN)$. From (29), z^* can also be written in terms of the packet loss requirement (p, x) as $z^* = -\frac{\log p}{x} \stackrel{\text{def}}{=} \xi$. Substituting (31) and (33) in (28) and setting $z = \xi$, we arrive at the following equation:

$$M\left(-\alpha-\beta+\sigma\xi+\sqrt{(\alpha+\beta-\sigma\xi)^2+4\beta\sigma\xi}\right)+ \\ N\left(-\lambda-\mu-\eta\xi c+\sqrt{(\lambda+\mu+\eta c\xi)^2-4\eta c\lambda\xi}\right)=0 \tag{34}$$

Let Ω be defined as follows:

$$\Omega \stackrel{\text{def}}{=} \frac{M\left(-\alpha-\beta+\sigma\xi+\sqrt{(\alpha+\beta-\sigma\xi)^2+4\beta\sigma\xi}\right)-N\left(\lambda+\mu\right)}{N}$$

Note that Ω is not a function of c, hence can be treated as a constant with respect to c. Equation (34) can now be written as:

$$\Omega-\eta\xi c+\sqrt{(\lambda+\mu+\eta\xi c)^2-4\eta\lambda\xi c}=0$$

Rearranging and squaring both sides of the above equation, we get

$$(\Omega-\eta\xi c)^2=\left[(\lambda+\mu+\eta\xi c)^2-4\eta\lambda\xi c\right] \tag{35}$$

Solving for c, we obtain a closed-form expression for the wireless EB c^*_{loss} subject to a packet loss constraint:

$$c^*_{loss}=\frac{\Omega^2-(\lambda+\mu)^2}{2\eta\xi(\mu-\lambda+\Omega)} \tag{36}$$

Next, we consider the delay case. From (30), we have $\Lambda_C(-z^*)=\frac{\log\epsilon_d}{t}\stackrel{\text{def}}{=}\vartheta$. Equating ϑ to the value of $\Lambda_C(-z^*)$ given in (32) and (33), we obtain

$$\vartheta=\frac{N}{2}\left(-\lambda-\mu-\eta cz^*+\sqrt{(\lambda+\mu+\eta cz^*)^2-4\eta\lambda cz^*}\right) \tag{37}$$

After some manipulations, the above equation can be expressed in terms of z^*:

$$z^*=-\frac{\frac{\vartheta^2}{N}+\vartheta(\lambda+\mu)}{\eta c(\vartheta+N\lambda)} \tag{38}$$

which gives z^* as a function of the channel parameters and the delay constraint. Likewise, z^* can be expressed in terms of the *source* parameters and the delay constraint: Substituting ϑ for $\Lambda_C(-z^*)$ in (28),

with $\Lambda_A(z^*)$ replaced by its value in (31), we obtain

$$-(\alpha+\beta)+\sigma z^*+\sqrt{(\alpha+\beta-\sigma z^*)^2+4\beta\sigma z^*}=-2\vartheta/M \tag{39}$$

which can be expressed in terms of z^*:

$$z^*=\frac{\frac{\vartheta}{M}\left(\frac{\vartheta}{M}-\alpha-\beta\right)}{\sigma\left(\beta-\frac{\vartheta}{M}\right)} \tag{40}$$

Equating (38) and (40), and solving for $c=c^*_{delay}$, we get a closed-form expression for the wireless effective bandwidth subject to a predefined delay constraint:

$$c^*_{delay}=\frac{\sigma M(\vartheta-\beta M)(\vartheta+N(\lambda+\mu))}{N\eta(\vartheta+N\lambda)(\vartheta-M(\alpha+\beta))} \tag{41}$$

5 Numerical Results

In this section, we provide numerical results obtained based on the previously presented analysis. A modulation scheme needs to be specified in order to obtain the BER curve and the corresponding service ratios. In our examples, we mostly focus on the binary phase-shift keying (BPSK) and the differential phase-shift keying (DPSK) modulation schemes. For BPSK modulation with coherent demodulation, the BER is given by:

$$P_e(r)=Q(\sqrt{2r}) \tag{42}$$

where r is the instantaneous received SNR and $Q(.)$ is the complementary error function. For DPSK modulation, the BER is given by:

$$P_e(r)=\frac{e^{-r}}{2} \tag{43}$$

In all of our examples, we let $n=424$ and $M=1$, and we use Reed-Solomon (RS) code for error correction. We also take $\epsilon^*=10^{-10}$ and $f_m=50$ Hz. Unless specified otherwise, we take $\rho=4$ and $\tau=5$ (hence $k=414$ for the RS code). The first two examples are intended to illustrate the partitioning approach. The first example uses BPSK modulation. Following the algorithm in Figure 4, we first obtain $r_N\approx 6.970$. From this value, we obtain $r_1=0.396$ and $N=2.9397$, which we truncate to three, i.e., the channel is represented by a 4-state FSMC. We then recompute the values of r_1 and λ/μ. The resulting

partition is given by:

$$(r_0, r_1, r_2, r_3, r_4) = (0, 0.396, 2.2284, 6.97, \infty)$$

with $\theta(\hat{r}_i) = i/3$ for $i = 0, \ldots, 3$. This partition is found adequate (i.e., it satisfies the service-ratio criterion).

For the second example, we consider DPSK modulation. In the first pass, we obtain $r_N = 6.6520$, $r_1 = 0.4425$, and $N = 2.7935$. Setting $N = 3$, we find that the resulting partition does not satisfy the required service ratios. Hence, we decrement N and recompute the calculations. For $N = 2$ the partition is given by:

$$(r_0, r_1, r_2, r_3) = (0, 0.4975, 6.6520, \infty)$$

with $\theta(\hat{r}_i) = i/2$ for $i = 0, 1, 2$. This partition is found to be appropriate.

Figure 5-a depicts $\theta(r)$ versus r for three different modulation schemes (BPSK, DPSK, and FSK). Their contrasting behavior indicates that the channel partitioning is dependent on the modulation scheme. Figure 5-b depicts $\theta(r)$ versus r for different values of τ with BPSK modulation. It can be noted that the larger the value of τ (stronger FEC code), the faster $\theta(r)$ approaches its asymptotic value, leading to a smaller value of N. As shown later, a larger N implies higher bandwidth allocation efficiency (less EB for a given QoS constraint). So one should always try to use the maximum possible N subject to the ability to enforce the requirements of the producer-consumer model. The impact of the choice of r_N on N is shown in Figure 6-a for different values of ρ (r_1 fixed at 1.0). It can be seen that there exists an "optimal" value for r_N at which N is maximized (and as shown later, the EB is minimized). Figure 6-b shows the variation of N as a function of r_1 for different values of ρ with r_N fixed at 9.70. From Figures 6-a and 6-b, it is clear that N depends on the separation between the thresholds r_1 and r_N (recall that for a given ρ, increasing r_N results in a smaller r_1). Figure 6-c shows the effect of ρ on N. It is observed that as ρ increases, so does N, suggesting the possibility of using ρ as a means of controlling N (since ρ can be controlled by adjusting the signal power at the transmitter).

Next, we study the impact of our channel partitioning approach on EB-based allocation subject to either a packet loss or a packet delay constraint. For brevity, we only show the results for BPSK modulation. The source parameters are set to $\sigma = 2604.1667$ packets/second (about 1.1 Mbps when using 424-bit packets), $\alpha^{-1} = 0.02304$ seconds, and $\beta^{-1} = 0.2304$ seconds. Unless noted otherwise, the results are obtained based on the previously described BPSK example with default parameter values for f_m, τ, and ρ. We vary most

of the remaining parameters and examine their impact on the EB.

Figure 7 depicts the impact of N on the EB. In theory, the channel partition, and subsequently the values of λ and μ, depend on N. However, in order to isolate the effect of N and gauge its impact on the EB separately from other factors, we fix λ and μ at their values in the BPSK example (with $N = 3$). For both the packet loss and delay cases, it is clear that for a given QoS constraint the EB decreases dramatically with an increase in N. This corroborates our intuition of the conservative nature of the popular two-state Markov channel model. For example, by using four states ($N = 3$) instead of two, c^*_{loss} subject to a PLR of 10^{-6} is reduced by almost 40% (and by 46% from the source peak rate). The reduction in the EB can be explained by the fact that characterizing the channel with a larger N reflects its error characteristics more accurately, and hence leads to more efficient allocation.

Figure 8 depicts the effective bandwidth as a function of the PLR constraint p using different buffer sizes (x) with $N = 3$. The figure shows that even with a small buffer, typical PLR requirements (e.g., 10^{-6} to 10^{-3}) can be guaranteed using an amount of bandwidth that is less than the source peak rate. The significance of our EB analysis is that it allows the network operator to decide beforehand the amount of resources (buffer and bandwidth) needed to provide certain QoS guarantees. A reduction in the per-connection allocated bandwidth translates into an increase in the network capacity (measured in the number of concurrently active mobile users). Figure 9 depicts a similar behavior for the delay case. In fact, the reduction in the required bandwidth is even more pronounced in this case.

Figure 10 depicts the wireless effective bandwidth versus the number of correctable bits (τ) for the delay and PLR cases. As τ increases, the EB decreases up to a certain point $\tau = \tau^*$, which one may call the "optimal" FEC. Beyond τ^* the trend is reversed (i.e., the overhead of FEC starts to outweigh its benefits).

Figure 11 demonstrates the impact of mobility on the effective bandwidth for the delay case ($t = 2$ seconds, $N = 3$, and $f_o = 1.9$ GHz). A change in the mobile speed (v) affects the Doppler frequency f_m, which in turn affects the level crossing rate $L(r)$. While $L(r)$ directly impacts the values of λ and μ, it does not impact the ratio λ/μ. Hence, the channel partitioning is not impacted by v. Interestingly, the EB is sensitive to v for small values of v. As the mobile speed exceeds a certain threshold, v barely impacts the EB. In this case, the channel becomes fast varying, stabilizing the amount of resources needed to ensure a specific level of QoS.

6 Conclusions

In this paper, we presented a new approach for partitioning the received SNR range that enables tractable analysis of the packet loss and delay performance over a time-varying wireless channel. This approach is based on adapting a multi-state embedded Markov channel model to Mitra's producer-consumer fluid model, which has known queueing performance. Our analysis exploited several properties of a slowly-varying wireless channel, including its level-crossing rate and the Rayleigh distribution of the signal envelope. We provided an algorithm for iterative computation of the various partitioning thresholds and the "nominal" BERs for the various states. We then investigated the wireless effective bandwidth subject to packet loss and delay constraints. Closed-form expressions were derived for the EB in each case. Besides capturing the channel fluctuations, our analysis also accommodates the inherent burstiness in the traffic through the use of appropriate fluid source models. Numerical examples showed that the allowable number of states (N) in the Markovian model depends on the underlying modulation scheme, the average SNR, and the separation between the thresholds r_1 and r_N. The larger the value of N, the higher is the channel efficiency (in terms of the EB). This observation establishes the true impact of the paper, as it demonstrates the conservative nature of the widely popular two-state model. The provided closed-form expressions for the EB can be used as part of admission control and service provisioning in cellular wireless packet networks.

Appendix

Dominant eigenvalue z^*

According to [14], z^* is the unique positive solution of (28). Replacing $\Lambda_A(z)$ and $\Lambda_C(-z)$ in (28) by their expressions in (31) and (32), respectively, we obtain:

$$\begin{aligned} &\tfrac{M}{2}\left(-\alpha-\beta+\sigma z+\sqrt{(\alpha+\beta-\sigma z)^2+4\beta\sigma z}\right)= \\ &-\tfrac{N}{2}\left(-\lambda-\mu-c_1 z+\sqrt{(\lambda+\mu+c_1 z)^2-4\lambda c_1 z}\right) \end{aligned} \tag{44}$$

After some straightforward algebraic manipulations, the above equation can be reduced into a cubic polynomial in z:

$$z(A_2 z^2 + A_1 z + A_0) = 0 \tag{45}$$

where

$$\begin{aligned}
A_2 &= \sigma^2(N/M)c_1\beta - \sigma c_1^2(N/M)^3\lambda + (N/M)^2 c_1\sigma(\lambda\sigma - \beta c_1) && (46)\\
A_1 &= \beta^2\sigma^2 + \lambda^2 c_1^2(N/M)^4 + (N/M)\beta\left[\sigma^2(\lambda+\mu) - c_1\sigma(\alpha+\beta)\right] && (47)\\
&\quad + \lambda c_1(N/M)^3\left[c_1(\alpha+\beta) - \sigma(\lambda+\mu)\right] && (48)\\
&\quad -2c_1\sigma(N/M)^2\left[\mu\beta + \lambda(\alpha+\beta)\right] && (49)\\
A_0 &= (\alpha+\beta)(\lambda+\mu)(\lambda c_1(N/M)^3 - \beta\sigma N/M) && (50)\\
&\quad + (N/M)^2\left[\lambda c_1(\alpha+\beta)^2 - \beta\sigma(\lambda+\mu)^2\right] && (51)
\end{aligned}$$

Clearly, $z = 0$ is one of the solutions to (45). The other two solutions, denoted by z_1 and z_2, are given by the roots of the quadratic polynomial in (45). Note that for a stable system, at least one of these two roots must be positive. Hence, if $z_1 < 0$, $z^* = z_2$. Otherwise, if both roots are positive, $z^* = \min\{z_1, z_2\}$.

References

[1] M. Zorzi, R. R. Rao, and L. B. Milstein, "Error statistics in data transmission over fading channels," *IEEE Trans. Commun.*, vol. 46, pp. 1468–1477, 1998.

[2] H. Bischl and E. Lutz, "Packet error rate in the non-interleaved Rayleigh channel,"*IEEE Trans. Commun.*, vol. 43, pp. 1375-1382, 1995.

[3] H. Steffan, "Adaptive generative radio channel models," *In Proceedings of the 5th IEEE International Symposium on Personal, Indoor and Mobile Radio Communications.*, vol. 1, pp. 268–273, 1994.

[4] S. Lin and D. J. Costello, *Error Coding: Fundamentals and Applications,* Englewood Cliffs, NJ: Printce Hall, 1984.

[5] W. C. Jakes, *Microwave Mobile Communications,* New York, NY: John Wiley & Sons, INC., 1977.

[6] B. Vucetic, "An adaptive coding scheme for time-varying channels," *IEEE Trans. Commun.*, vol. 39, pp. 653–663, May 1991.

[7] M. Rice and S. B. Wicker, "Adaptive error control for slowly-varying channels," *IEEE Trans.Commun.*, vol. 42, pp. 917-925,1994.

[8] H.S. Wang and N. Moayeri, "Finite-state Markov Channel- a useful model for radio communication channels," *IEEE Trans. Vech. technol.*, vol. 44, pp. 163–171, 1995.

[9] Q. Zhang and Salem A. Kassam, "Finite-state Markov model for Rayleigh fading channels," *IEEE Trans. Commun.*, vol. 47, Nov. 1999.

[10] Y. L. Guan and L. F. Turner, "Generalized FSMC model for radio channels with corrlated fading," *IEEE Proc. Commun.*, vol. 146, April. 1999.

[11] J. Kim, and M. Krunz,"Bandwidth allocation in wireless networks with guaranteed packet-loss performance," *IEEE/ACM Transactions on Networking*, vol. 8, pp. 337-349, 2000.

[12] V. S. Frost and B. Melamed,"Traffic Modeling for Telecommunications Networks," *IEEE Communications Magazine*, vol. 32, pp. 70–81, Mar. 1994.

[13] J. Kim, and M. Krunz,"Delay analysis of selective repeat ARQ for a Markovian source over a wireless channel," *IEEE Transactions on Vehicular Technology*, vol. 49, pp. 1968-1981, Sep. 2000.

[14] C.-S. Chang, *Performance Guarantees in Communication Netwoks,* London Berlin Heidelberg: Springer-Verlag, 2000.

[15] M. Krunz, and J. Kim,"Fluid analysis of delay and packet discard performance for QoS support in wireless networks ," *IEEE Transactions on Selected Areas in Communications*, vol. 19, pp. 384-395, Feb 2001.

[16] D. Mitra,"Stochastic theory of a fluid model of producers and consumers coupled by a buffer," *Adv. Appl. Prob.*, vol. 20, pp. 646-676, 1988.

[17] D. Anick, D. Mitra, and M. M. Sondhi,"Stochastic theory of a data–handling system with multiple sources,"*Bell Syst. Tech. J.*, vol. 61, pp. 1871–1894, Feb. 1982.

[18] A. I. Elwalid and D. Mitra, "Effective bandwidth of general Markovian traffic sources and admission control of high speed networks, "*IEEE/ACM Trans. Networking*, vol. 1, pp. 329–343, 1993.

[19] A. Elwalid, D. Heyman, T. V. Lakshman, D. Mitra, and A. Weiss, "Fundamental bounds and approximations for ATM multiplexers with applications to video teleconferencing, "*IEEE J. Select. Areas Commun., vol. 13, pp. 1004–1016*, 1995.

[20] A. I. Elwalid, and D.Mitra, "Statistical multiplexing with loss priorities in rate-based congestion control of high-speed networks,"*IEEE Trans. Commun.*, vol. 42, pp. 2989–3002,1994.

[21] A. Mohammadi, S. KuMar, and D. Klynmyshyn, "Characterization of effective bandwidth as a metric of quality of service for wired and wireles ATM networks," *IEEE ICC*, vol. 2, pp. 1019–1024, 1997.

[22] R. Guérin, H. Ahmadi, and M. Naghshineh, "Equivalent capacity and its application to bandwidth allocation in high-speed networks," *IEEE J. Select. Areas Commun.*, vol. 9, no. 7, pp. 968–981, Sep. 1991.

[23] R. J. Gibbens and P. J. Hunt, "Effective bandwidths for the multi-type UAS channel," *Queueing Syst.* vol. 9, pp. 17–28, 1991.

[24] N. Guo and S. D. Morgera, "Frequency-hopped ARQ for wireless network data services," *IEEE J. Select. Areas Commun.*, vol. 12, no. 8, pp. 1324–1336, Sep. 1994.

[25] F. P. Kelly,"Effective bandwidths at multi-type queues," *Queueing Syst.* vol. 9, pp. 5–15, 1991.

[26] G. L. Choudhury, D. M. Lucatoni, and W. Whitt, "Squeezing the most out of ATM," *IEEE Trans. Commun.*, vol. 44, no. 2, pp. 203–217, Feb. 1996.

[27] P G. Hoel, S. Port, and C. Stone, *Introduction to Stochastic Processes,* Prospect Heights, IL: Waveland Press, Inc., 1972.

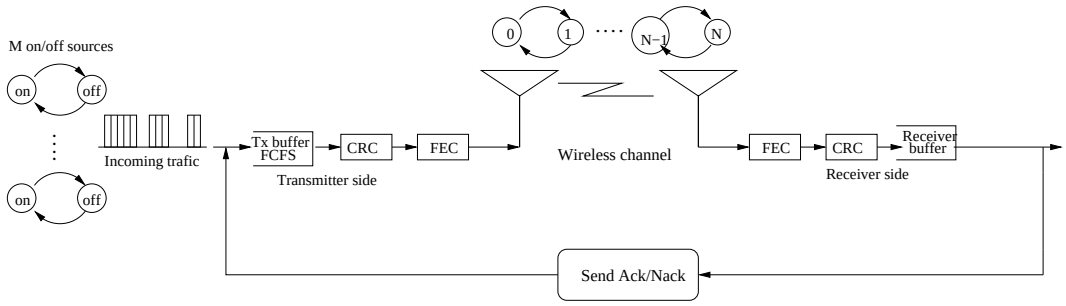

Figure 1: Wireless-link model.

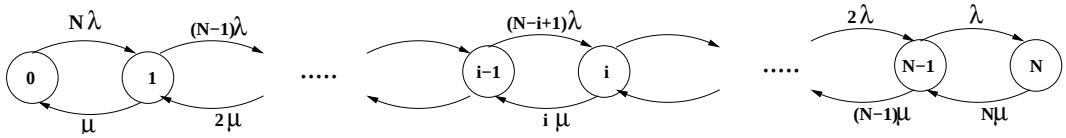

Figure 2: Markov chain in Mitra's producer-consumer model.

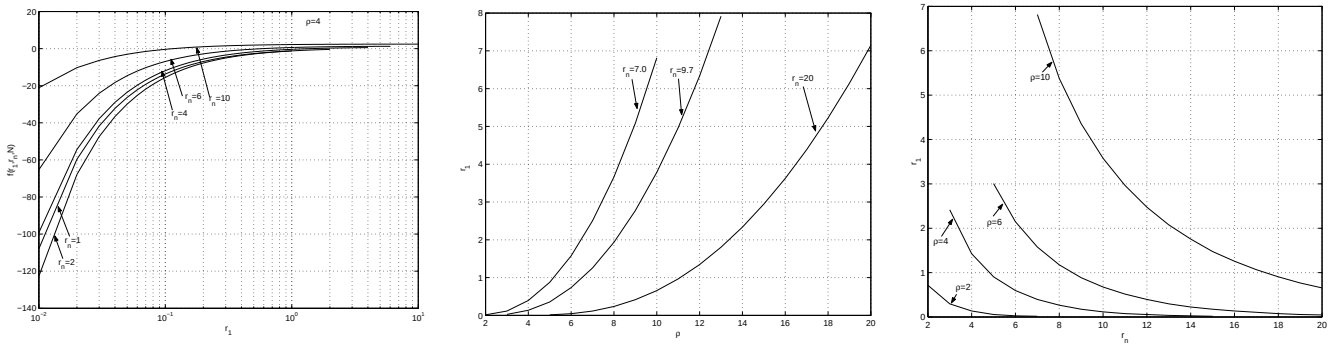

(a) $f(r_1, r_N, N)$ versus r_1 for different values of r_N ($\rho = 4$).

(b) r_1 versus ρ for different values of r_N.

(c) r_1 versus r_N for different values of ρ.

Figure 3: Behavior of r_1, r_N, and ρ.

Parameterize-FSMC$(\rho, P_e(.), \epsilon^*, n, \tau)$
1. Choose an appropriate r_N by solving (21)
2. Solve (19) numerically for r_1 with N replaced by (20)
3. Calculate N using (20)
4. Set $N = \lceil N \rceil$
5. Recompute r_1 using (19)
6. Recompute λ/μ using (17)
7. Solve for the remaining thresholds as follows:
   for i=1, ..., $N-2$
   $\pi_i = \begin{pmatrix} N \\ i \end{pmatrix} (\frac{\lambda}{\mu})^i (1 - e^{\frac{-r_1}{\rho}})$
   $r_{i+1} = -\rho \ln(e^{\frac{-r_i}{\rho}} - \pi_i)$
   end for
8. Check for the *existence* of appropriate nominal SNR values:
   for i=1, ..., $N-1$
   if $\theta(r_i) \leq i/N$, **continue**
   else /* partitioning is not appropriate */
   set $N = N - 1$
   if $N = 1$
   return 2-state GE solution
   else goto step 5
   end if
   end if-else
   end for
9. Compute the nominal SNR values:
   for i=1, ..., $N-1$
   Solve $\theta(\hat{r}_i) = \frac{i}{N}$ numerically for $\hat{r}_i$
   end for
10. **return**$(N, r_1, \ldots, r_N, \hat{r}_1, \ldots, \hat{r}_{N-1})$

Figure 4: Algorithm to calculate the parameters of the FSMC model.

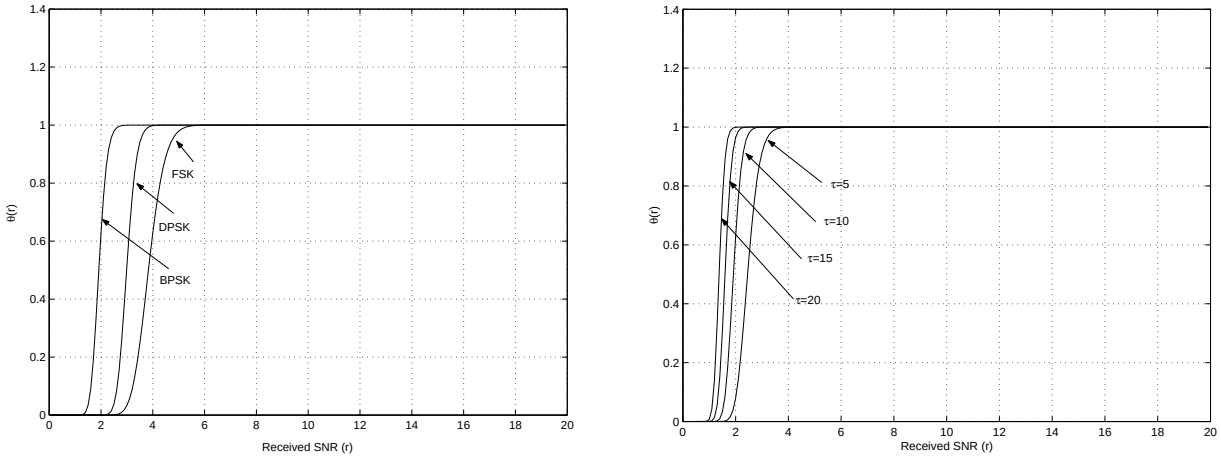

(a) Different modulation schemes ($\tau = 5$). (b) Different correction capabilities (BPSK).

Figure 5: Service ratio $\theta(r)$ versus r.

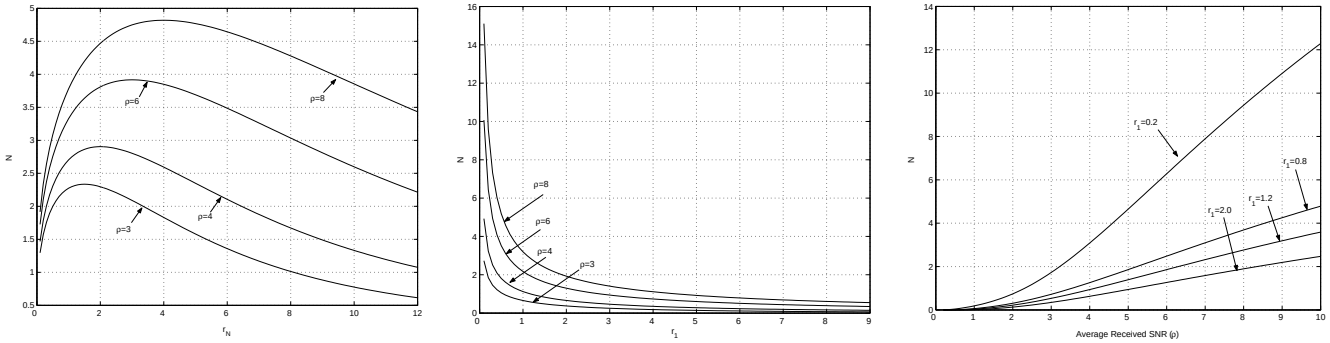

(a) N versus r_N for different values of ρ (r_1=1.0).

(b) N versus r_1 for different values of ρ (r_N =9.7).

(c) N versus average received SNR ρ (r_N =9.7).

Figure 6: N versus key channel parameters ρ, r_1, and r_N.

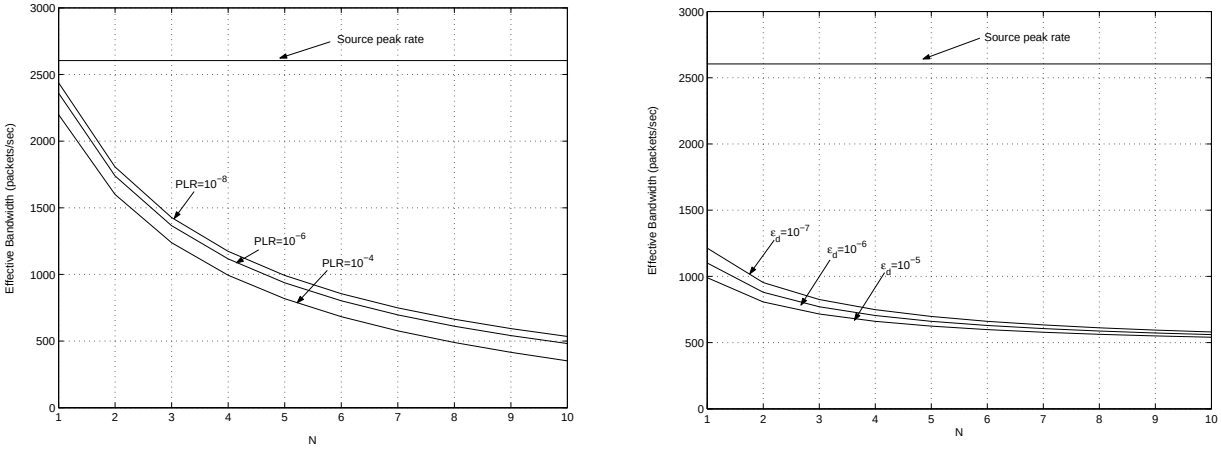

(a) c^*_{loss} (buffer size = 50).

(b) c^*_{delay} (t = 2 msec).

Figure 7: Effective bandwidth versus N.

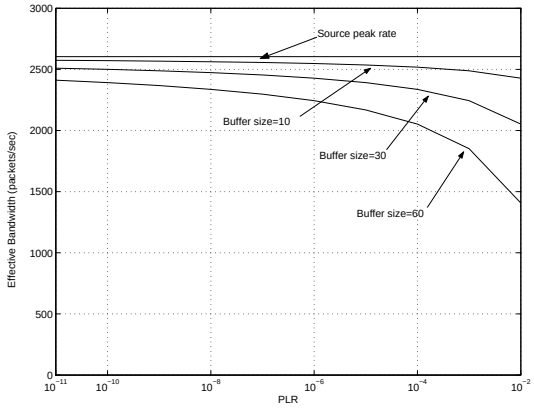

Figure 8: c^*_{loss} versus the PLR p ($N = 3$).

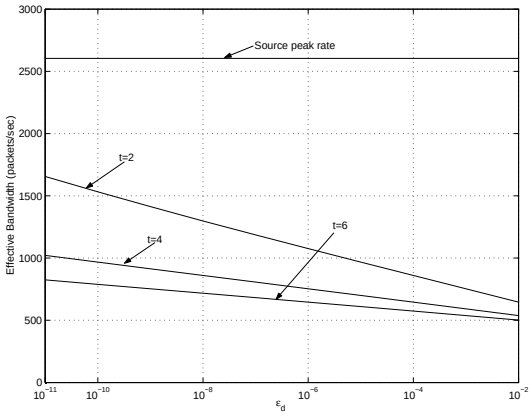

Figure 9: c^*_{delay} versus ϵ_d ($N = 3$).

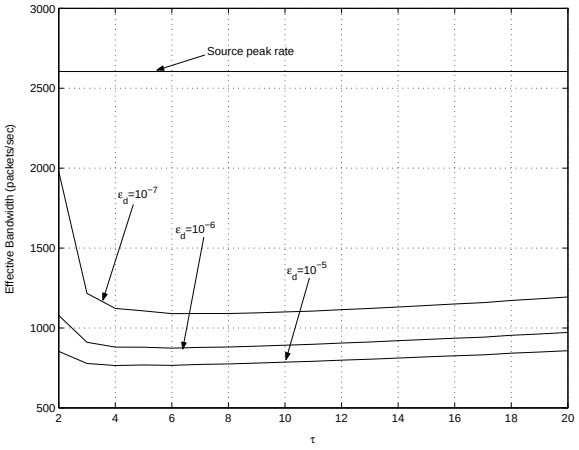

(a) c^*_{delay} ($t = 1$).

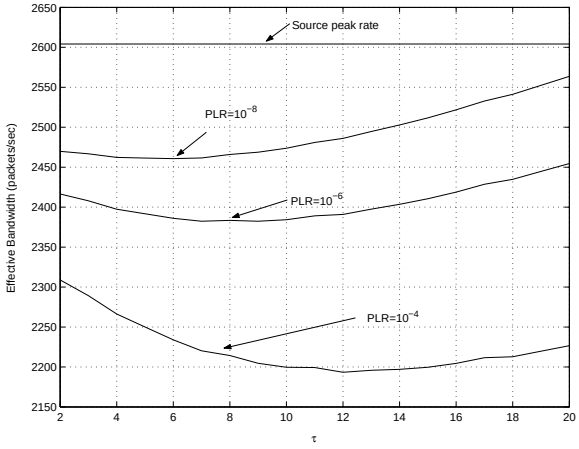

(b) c^*_{loss} (buffer size = 50).

Figure 10: Effective bandwidth versus the number of correctable bits (τ).

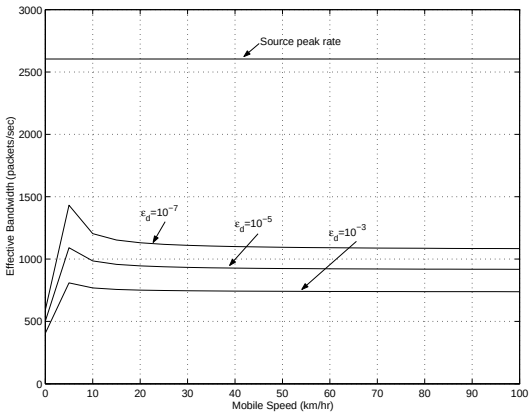

Figure 11: c^*_{delay} versus mobile speed (v).